Ion acoustic wave generation by a standing electromagnetic field in a subcritical plasma

P. Fischer, C. Gauthereau, J. Godiot, G. Matthieussent

Classification
Physics Abstracts
52.35

Ion acoustic wave generation by a standing electromagnetic field in a subcritical plasma

P. Fischer, C. Gauthereau (+), J. Godiot and G. Matthieussent

Laboratoire de Physique des Gaz et des Plasmas (++),
Greco I.L.M.-Greco Plasma, Université Paris Sud, 91405 Orsay, France

(*Reçu le 30 octobre 1985, révisé le 13 juin 1986, accepté le 30 septembre 1986*)

Résumé. — Une onde électromagnétique ($f = 9$ GHz, $P_i = 150$ kW, $\tau = 1.5$ μs) est excitée dans un plasma sous-critique ($n_e \simeq 10^{11}$ cm^{-3}, $P_0 \simeq 5 \times 10^{-4}$ Torr) et y produit une onde stationnaire. La force pondéromotrice, associée à cette onde stationnaire, excite une onde acoustique ionique de vecteur d'onde double de celui de l'onde électromagnétique et avec une fréquence ($f_A \simeq 150$ kHz) satisfaisant l'équation de dispersion habituelle. Les caractéristiques essentielles de l'onde acoustique ionique, mesurées dans cette expérience 3D, sont en accord avec un modèle simple. Cependant le spectre des ondes acoustiques ioniques fait apparaître des sous-harmoniques lorsque la densité du plasma varie.

Abstract. — An electromagnetic wave ($f = 9$ GHz, $P_i = 150$ kW, $\tau = 1.5$ μs) is launched into a subcritical argon plasma ($n_e \simeq 10^{11}$ cm^{-3}, $P_0 \simeq 5 \times 10^{-4}$ Torr), resulting in a standing wave. The associated ponderomotive force generates an ion acoustic wave with a wave vector equal to twice the electromagnetic one and with a frequency satisfying the usual dispersion relation ($f_A \simeq 150$ kHz). The main features of the ion acoustic wave, as measured in this 3D experiment, agree with a simple theory. However, varying the plasma density, the ion acoustic spectrum reveals a non-linear feature, i.e. the existence of subharmonics.

1. Introduction.

Our purpose is to study the ion acoustic wave excited in a subcritical plasma by the ponderomotive force [1] associated with a standing electromagnetic pulse. Because of the nonlinear response of the plasma to the electromagnetic pulse, a zero frequency electron density perturbation is created with a wave number twice the electromagnetic one. Then, after the pulse, the plasma relaxes towards equilibrium, emitting ion acoustic waves which verify the usual dispersion relation [2].

Stimulated Brillouin backscattering [3], already observed in laser fusion experiments and in microwave interaction with plasma [4], is not present in this experiment : the electromagnetic pulse length is shorter than the inverse of the instability growth rate.

Thus experimental results concerning the nonlinear excitation of the ion acoustic waves and its linear propagation are given and compared with an elementary theory.

2. The experiments.

The experiments were performed in a great volume (0.8 m^3) of unmagnetized plasma, produced in a multipolar discharge [5]. Typical operating parameters were gas filling pressure (Argon) : $P_0 \simeq 5 \times 10^{-4}$ Torr, electron density : $n_e \simeq 10^{11}$ cm^{-3}, electron temperature : $T_e \simeq 3$ eV. With these conditions, the ion-neutral collision frequency was $\nu_{in} \simeq 10^4$ s^{-1}. The plasma density gradient could be modified by moving a mica sheet disposed transversally to the longitudinal discharge axis (x axis) [5, 6]. The characteristic gradient length,

$$L \equiv \left[\frac{1}{n_e}\frac{dn_e}{dx}\right]^{-1} \quad (1)$$

was thus adjustable between 10 m (uniform plasma) and 0.5 m (nonuniform plasma). In addition, the mica

(+) Now at DPC-IRDI-CEN Saclay, 91191 Gif-sur-Yvette, France.

(++) Laboratory associated with the CNRS.

sheet insured homogeneous boundary conditions both for plasma and for microwaves : the radial (y axis) density gradient was always comparable with the longitudinal gradient obtained without the mica sheet ($L \simeq 10$ m).

The electromagnetic wave was launched by a horn along the x axis with a frequency $\omega_0/2\pi = 9$ GHz, pulse width $\tau = 1.5$ μs and peak power up to 150 kW (Fig. 1). This wave was reflected by the chamber end wall. We will express the forward and reflected fields as

$$E_i = E_0 \sin\left(\omega_0 t - k_0 x\right)\left[Y(t) - Y(t-\tau)\right] \quad (2)$$

and

$$E_r = r^{1/2} E_0 \sin\left(\omega_0 t + k_0 x\right)\left[Y(t) - Y(t-\tau)\right] \quad (3)$$

where $Y(t)$ is the Heaviside step function, r the reflection coefficient ; k_0 is the wave vector and satisfies the dispersion relation (ω_p is the plasma frequency) :

$$k_0 = \frac{\omega_0}{C}\left(1 - \frac{\omega_p^2}{\omega_0^2}\right)^{1/2}. \quad (4)$$

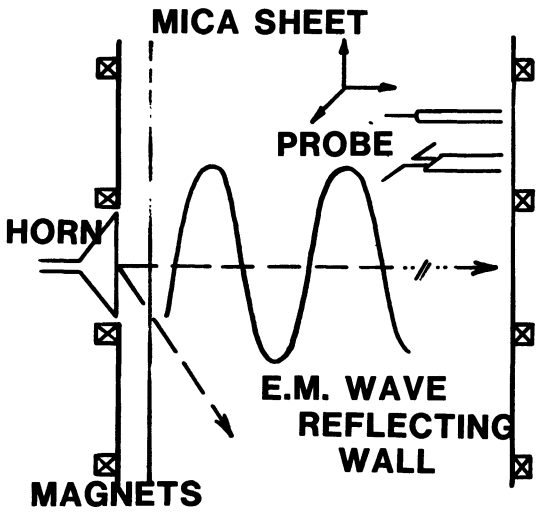

Fig. 1. — Experimental set up. Electromagnetic wave launching and detection.

The combination of the incident and reflected fields resulted in a standing wave with wave number equal to $2k_0$. The reflection coefficient was obtained by a measurement of the standing wave ratio, θ, by the relations

$$\theta = \frac{E_{max}}{E_{min}} \quad (5)$$

$$r = \left[\frac{\theta - 1}{\theta + 1}\right]^2. \quad (6)$$

Electromagnetic measurements were performed with a movable dipole antenna associated either with an interferometer or a quadratic detector. As can be seen in figure 2, the surfaces of constant phase are planes roughly perpendicular to the x axis. Figure 3 gives the reflection coefficient. It varies from 0.05 in the neighbourhood of the horn to 0.15 at about 20 cm.

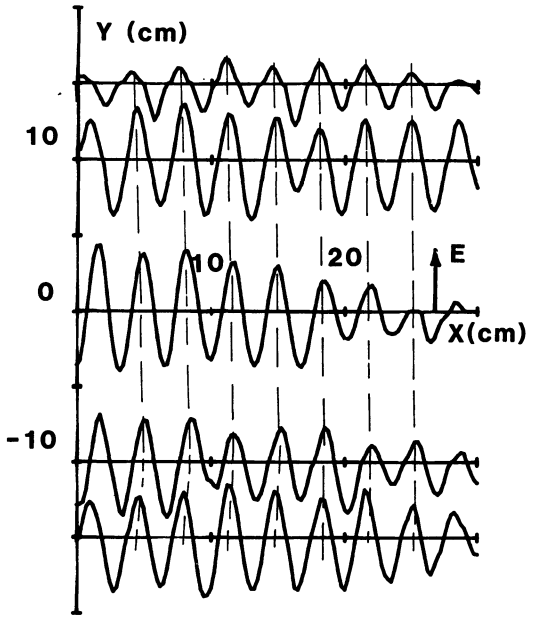

Fig. 2. — Output of the interferometer as a function of the distance along the longitudinal axis of the device (X) for different values of the radial position (Y). The dotted lines show the phase plane of the electromagnetic wave.

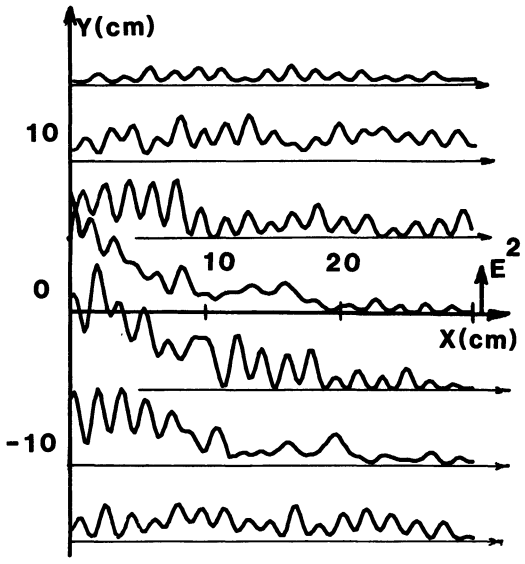

Fig. 3. — Output of the quadratic detection system. Same representation as figure 2.

3. Results and interpretation.

In the presence of the standing wave, plasma electrons suffer a zero frequency ponderomotive force [1],

$$\mathbf{F} = -\frac{1}{2}\frac{e^2}{m\omega_0^2}\nabla\left\langle \left(E_i + E_r\right)^2\right\rangle, \qquad (7)$$

where the brackets denote a time average. Using (2) and (3) this expression becomes

$$\mathbf{F} = -\frac{1}{4}\frac{e^2}{m\omega_0^2}\nabla\left[2\,r^{1/2}E_0^2\cos\left(2\,k_0 x\right)\right] \times \times \left[Y(t) - Y(t-\tau)\right]. \qquad (8)$$

This force, which derives from a potential U, induces a pertubation of the electron density, δn_0, which can be written

$$\frac{\delta n_0}{n_0} \simeq -\frac{U}{KT_e}. \qquad (9)$$

Using this as a source term in the ion acoustic wave equation we obtain [4]

$$\left[\frac{\partial^2}{\partial t^2} - C_s^2\frac{\partial^2}{\partial x^2}\right]\frac{\delta n}{n_0} = -k_0^2 C_s^2\frac{v_0^2}{v_e^2}2\,r^{1/2}\cos\left(2\,k_0 x\right) \times \times \left[Y(t) - Y(t-\tau)\right] \qquad (10)$$

where n_0 is the equilibrium plasma density, δn the plasma density perturbation, v_0 the maximum electron oscillating velocity in the electromagnetic field, v_e, the electron thermal speed

$$v_e = \left(\frac{k_B T_e}{m_e}\right)^{1/2} \qquad (11)$$

and C_s, the ion acoustic velocity

$$C_s = \left(\frac{k_B T_e}{m_i}\right)^{1/2}. \qquad (12)$$

Thus, the ion acoustic wave vector, k_A, is twice the electromagnetic one and the frequency, ω_A, satisfies the usual dispersion relation,

$$\omega_A = \pm 2\,k_0 C_s. \qquad (13)$$

Using a fine cylindrical Langmuir probe biased a few volts above plasma potential, we detected the ion acoustic waves after the end of the electromagnetic pulse. Having checked that the electron temperature does not vary significantly immediately after the pulse, we can safely assume that the electron saturation current variations are proportional to plasma density fluctuations. Figure 4 shows, at a fixed point, the temporal evolution of both the electromagnetic intensity and the induced plasma density perturbation : the

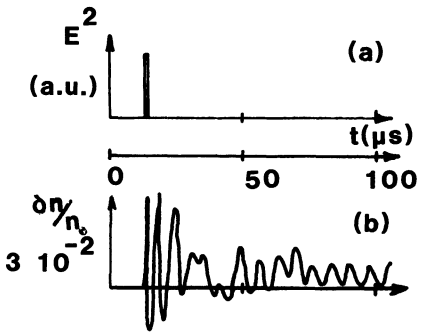

Fig. 4. — Amplitude of the electromagnetic wave and density perturbation measured by a Langmuir probe, as a function of time.

observed ion acoustic wave frequency is thus $\omega_A/2\,\pi = 150$ kHz, which implies

$$\tau \ll \left(\frac{\omega_A}{2\,\pi}\right)^{-1}. \qquad (14)$$

With this condition and including a collisional damping, the solution of equation (10) can be written

$$\frac{\delta n}{n_0} \simeq -\frac{1}{4}\frac{v_0^2}{v_e^2}r^{1/2}\,\omega_A\,e^{-\nu_{in}t} \times \times \left[\sin\left(\omega_A t + 2\,k_0 x\right) + \sin\left(\omega_A t - 2\,k_0 x\right)\right]. \qquad (15)$$

To sum up, the ponderomotive force associated with the standing electromagnetic wave creates a zero frequency electron density perturbation with a fixed wave vector. Then, after the end of the pulse, the plasma relaxes towards equilibrium, emitting two ion acoustic waves which propagate in opposite directions.

Time flying measurements (Fig. 5) show that this is indeed the case. These measurements are performed on the maximum or minimum amplitude of the electron density perturbation for distances much less than a wavelength and allow to distinguish the two opposite directions of propagation. The observed phase velocity is within 10 % of the ion acoustic velocity (12), calculated with the electron temperature obtained from a Langmuir probe. The wavelength is given by equation (13), using the observed frequency and phase velocity. We found half the electromagnetic wavelength measured by interferometry, to within 15 %.

Nevertheless, in contrast to (15), we found that the relative amplitudes of the two oppositely propagating waves change in time. This disagreement may be due to the fact that the reflection coefficient varies from point to point.

In order to confirm the nature of the excited waves, time flying measurements were done for various electronic temperatures at constant plasma density : the argon pressure was varied from 3×10^{-4} to 10^{-3} Torr

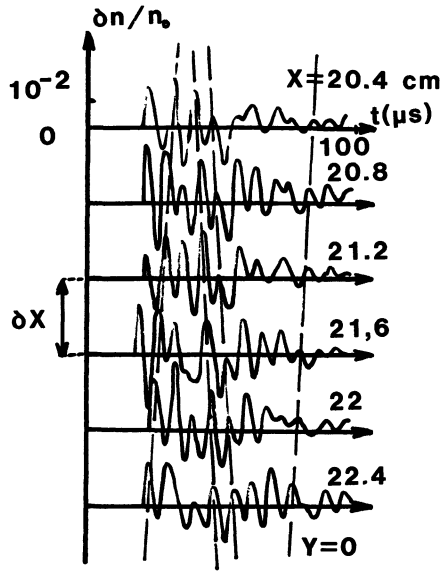

Fig. 5. — Time of flight measurements. Measurements are performed along the axis of the device ($Y = 0$) and for each position (X) of the probe, the ion acoustic signal is plotted as a function of time. The vertical shift of each signal is proportional to the distance along which the probe has been moved. The slope of the dotted line is the propagation velocity of the ion acoustic wave.

and the discharge current adjusted. By so doing, the ratio of the wave frequency to the electron temperature square root should remain constant :

$$\frac{\omega_A}{2\pi\sqrt{k_B T_e}} = \sqrt{\frac{e}{m_i}}\frac{k_0}{\pi}. \qquad (16)$$

Figure 6 shows that this is clearly the case.

The amplitude of the relative density perturbation is given by, (15) :

$$\left|\frac{\delta n}{n_0}\right| = \frac{1}{2}\frac{v_0^2}{v_e^2} r^{1/2}\omega_A \tau . \qquad (17)$$

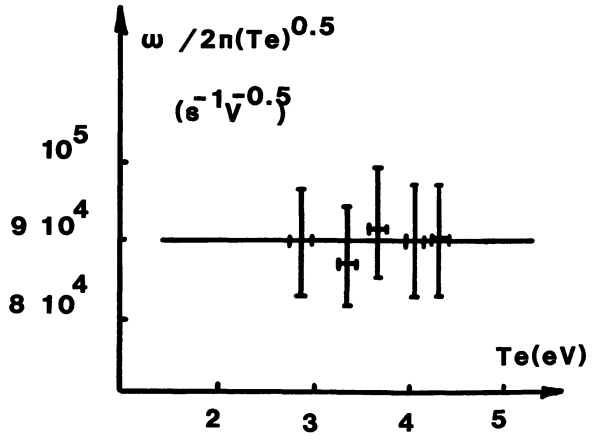

Fig. 6. — Ion acoustic wave dispersion relation, the parameter is the electron temperature.

The area illuminated by the microwave horn was, at 20 cm where the measurements were performed, on the order of 400 cm^2 (Fig. 3). The oscillating electron velocity was then about 0.2 times their thermal velocity and (17) gives a relative density perturbation of about 1 %, which is in agreement with the experimental results.

From equations (15) and (17), other previsions can be deduced and checked : with a short electromagnetic pulse and at a fixed point, the ion acoustic signal shape should be independent of pulse length τ, but the density perturbation amplitude should be proportional to τ. This can be clearly seen in figures 7 and 8.

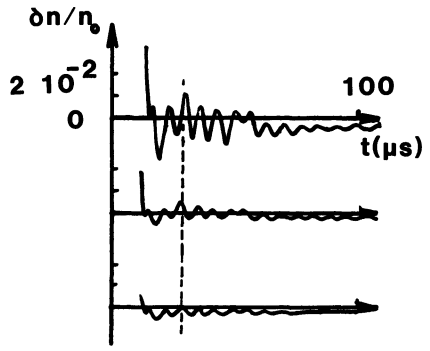

Fig. 7. — Ion acoustic perturbation for different high frequency pulse lengths.

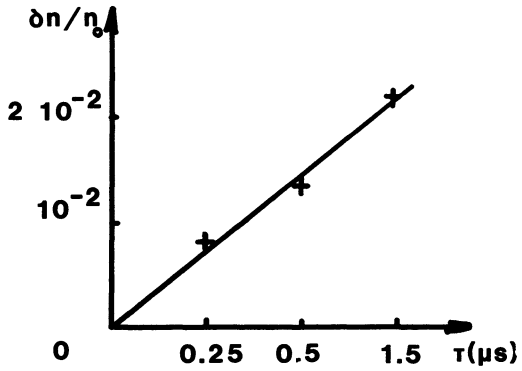

Fig. 8. — Relative density perturbation of the ion acoustic wave as a function of the pulse length.

Figure 9 gives the ion acoustic signal Fourier spectrum. It has been obtained by applying a fast Fourier transform to the waveform acquired on a digital storage oscilloscope. This was necessary because spectrum analysis by analogical means was made unpractical by low frequency noise generated by the magnetron.

When a density gradient is created in the plasma by a mica sheet, we observe a splitting of the fundamental frequency. This can be explained by a Doppler effect :

$$\omega_A = 2k_0\left(C_s \pm v_D\right) \qquad (18)$$

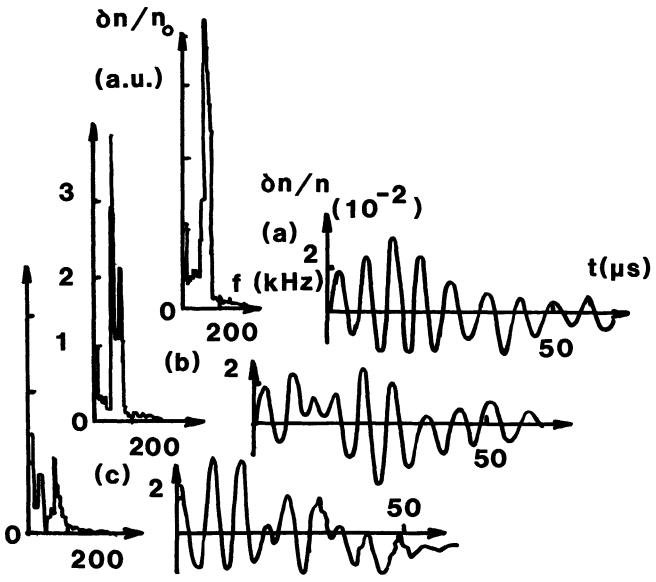

Fig. 9. — Ion acoustic wave spectrum and corresponding density perturbation for a) a homogeneous plasma ($L \simeq 10$ m) ; b) a plasma with a weak gradient ($L \simeq 2$ m) ; c) a plasma with a strong gradient ($L \simeq 0.5$ m).

where v_D is the plasma drift velocity along the discharge axis, towards the mica sheet, and which is related to the gradient length, L, by

$$v_D = \frac{k_B T_e}{m_i \nu_{in}} \frac{1}{L}. \tag{19}$$

For example, when the mica sheet was at one cm of the end of the device, and with the same experimental conditions as above, the two frequencies were 127 and 170 kHz. The electron temperature and drift velocity obtained from (18) are then respectively 3 eV and 3.6×10^2 m/s, which is in agreement with the electron temperature and gradient length, $L \simeq 2$ m, obtained by a Langmuir probe.

When the plasma becomes strongly inhomogeneous ($L \lesssim 1$ m), the two peaks merge into a single broad one ($\Delta\omega_A/2\pi \simeq 50$ kHz) and the amplitude decreases with increasing inhomogeneity.

When the uniform plasma density is varied around 10^{11} cm^{-3}, for discrete values of this parameter, in addition to the fundamental frequency of the ion acoustic wave f_0, as predicted by the simple model, the spectrum shows the existence of subharmonics. Such a behaviour can be interpreted as the beginning of a transition towards turbulence by period doubling in a system subject to resonant mode coupling [7].

Figure 10 shows that, for a density of 1.2×10^{11} cm^{-3}, the frequencies f_0, $\frac{1}{2}f_0$, $\frac{1}{4}f_0$ are present in the system and for a density of 1.6×10^{11} cm^{-3} these are f_0, $\frac{2}{3}f_0$ and $\frac{1}{3}f_0$. Between these two values of the density the spectrum exhibits the usual frequency f_0, excited by the ponderomotive force.

A simple estimate from mode coupling theory, neglecting the dispersion of the ion acoustic wave, gives the characteristic time of appearance of the half harmonic $t_{1/2}$ as

$$t_{1/2} = \frac{2}{\omega_A \dfrac{\delta n}{n}}$$

with the experimentally measured parameters, this leads to a time of the order of a few hundred of microseconds. This characteristic time, of the same order as the collision time ν_{in}^{-1}, seems too long to explain the appearance of subharmonic frequencies.

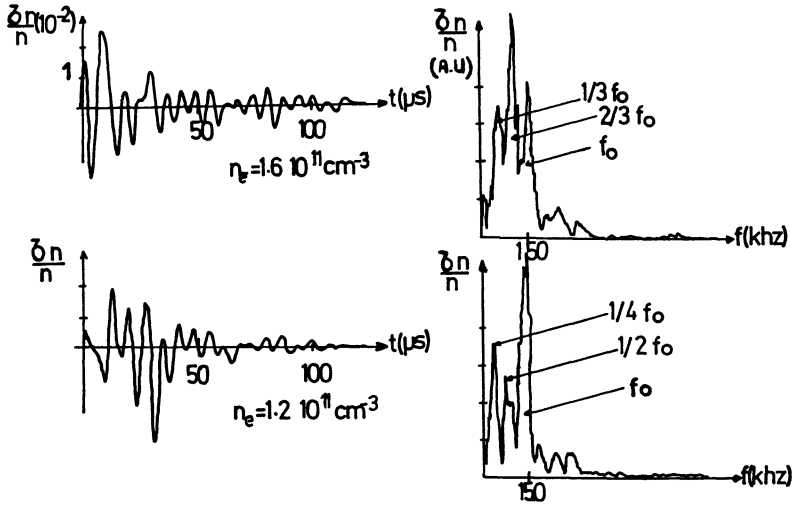

Fig. 10. — Density perturbation and ion acoustic wave spectrum for different values of the zero order density.

4. Conclusion.

We reported the generation of ion acoustic waves by the ponderomotive force of a standing electromagnetic wave, in a subcritical plasma.

The main features of these waves have been compared with the predictions of a simple theory and good agreement is found. However, the usual mode coupling theory does not seem to account for the appearance of subharmonics of the excited ion acoustic wave when the plasma density is varied.

Acknowledgments.

This work was supported in part by the DRET. The authors are also indebted to Thomson-CSF for the loan of a magnetron with its modulator.

References

[1] MAX, C. E., in *Laser Plasma Interaction*, Les Houches, Session XXXIV, edited by R. Balian, J. C. Adam (North-Holland) 1980, p. 301 ; PELLAT, R., *Ibidem*, p. 411.

[2] MONTES, C., *Phys. Rev. Lett.* **50** (1983) 1129.

[3] PHILLION, D. W., KRUER, W. L., RUPERT, V. C., *Phys. Rev. Lett.* **39** (1977) 1529.

[4] HUEY, H. E., MASE, A., LUHMANN, N. C., DIVERGILIO, W. E., THOMSON, J. J., *Phys. Rev. Lett.* **45** (1980) 795.

[5] BENHASSINE, M., BOURDESSOL, J. C., GAUTHEREAU, C., GODIOT, J., MATTHIEUSSENT, G., RAUCH, J. L., *Revue Phys. Appl.* **19** (1984) 545.

[6] GAUTHEREAU, C., MATTHIEUSSENT, G.; RAUCH, J. L., GODIOT, J., *Phys. Lett.* **101A** (1984) 394.

[7] BUSSAC, M. N., *Physica Scripta* **2** (1982) 110.